Desalination and Water Treatment
www.deswater.com

doi: 10.5004/dwt.2017.20373

67 (2017) 324–331
March

Photocatalytic performance of chromium-doped TiO_2 nanoparticles for degradation of Reactive Black 5 under natural sunlight illumination

B. Shahmoradi[a,*], M. Pirsaheb[b], M.A. Pordel[a], T. Khosravi[b],
Radheshyam R. Pawar[c], Seung-Mok Lee[c,*]

[a]*Environmental Health Research Center, Kurdistan University of Medical Sciences, Sanandaj, Iran, Tel. +98-9187705355; Fax: +98-87-33625131; emails: bshahmorady@gmail.com, bshahmoradi@muk.ac.ir (B. Shahmoradi), mapordel1@gmail.com (M.A. Pordel)*
[b]*Research Center for Environmental Determinants of Health (RCEDH), Kermanshah University of Medical Sciences, Kermanshah, Iran, emails: mpirsaheb@yahoo.com (M. Pirsaheb), toubakhosravi@gmail.com (T. Khosravi)*
[c]*Department of Energy and Environment Convergence Technology, Catholic Kwandong University, 522 Naegok-dong, Gangneung 210-701, Korea, Tel. +82-33-649-7535; Fax: +82-33-642-7635; email: leesm@cku.ac.kr (S.-M. Lee)*

Received 22 June 2016; Accepted 19 November 2016

ABSTRACT

Azo dyes are widely used in textile industries throughout the world. Discharging partially treated or untreated effluents of such industries can bring about environmental issues in receiving water bodies. The present investigation focuses on synthesis, characterization, and degradation application of chromium-doped TiO_2 nanoparticles. The mild hydrothermal synthesis protocol was applied for the preparation of chromium-doped TiO_2 nanoparticles. Nanoparticles fabricated were characterized using X-ray diffraction, scanning electron microscopy, energy dispersive X-ray analysis, and attenuated total reflection analysis techniques. The characterization results confirmed the successful doping of chromium, and textural properties results reveal higher crystallinity, spherical morphology, and excellent purity of Cr-doped TiO_2 nanoparticles. The photodegradation efficiency of chromium-doped TiO_2 was investigated for the treatment of hazardous Reactive Black 5 dye from aqueous solution. The degradation efficiency was systematically optimized through varying operational parameters including dopant mol% ratio (1, 1.5, and 2 mol%), influence of solution pH (4, 7, and 10), nanomaterial dosage (0–5 g/L), dye concentration (10–300 mg/L), H_2O_2 concentration (5–50 mmol/L), and contact time (0–120 min) under natural sunlight illumination. The catalytic performance was highly improved due to 1 mol% Cr-doping, at pH 4, 20 mmol/L of H_2O_2, 5.0 g/L of nanomaterial dosage, and 120 min of contact time where maximum degradation efficiency was achieved to 96.6% (50 mg/L Reactive Black 5 dye) under sunlight illumination.

Keywords: Chromium-doped TiO_2; Reactive Black 5; Sunlight; Photodegradation; Hydrothermal; Nanostructure

1. Introduction

Synthetic dyes, particularly azo dyes, are growing rapidly in different dye using industries [1–4]. The world annual production of dyes is estimated at more than 80,000 tons used mainly in food industries, cosmetics, paper mills, and especially in textile industries, which alone absorb more than 70% of the produced total quantity [5,6]. These crucial organic compounds are not only inducing color to the receiving water bodies but are also potentially toxic to the human being and environment [7]. This creates an aesthetic pollution problem and is a major perturbation to aquatic life; reducing autopurification capacity of receiving systems [8]. C.I. Reactive Black 5 (RB5; Table 1) is one of the representative diazo dyes found in textile wastewaters [9,10]. They are lethal, hazardous, and

---

* Corresponding author.

Table 1
Characteristics of Reactive Black 5 dye

Chemical structure	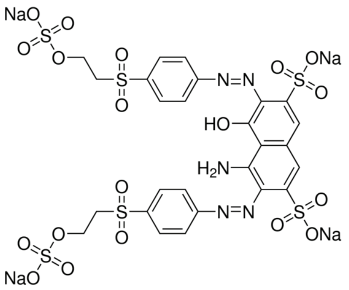
CAS number	17095-24-8
Synonym	Remazol Black B, Begazol Black B
Empirical formula	$C_{26}H_{21}N_5Na_4O_{19}S_6$
Molecular weight	991.82

carcinogenesis contaminants classified as one of the foremost pollutants in United State Environmental Protection Agency list with a limit of discharge less than 0.5 ppm [11,12]. In most cases, these dyes are partially treated and released into the environment without proper treatment. Conventional methods such as chemical precipitation and biological treatment cannot effectively remove dyes from effluents; therefore, finding an effective technique is necessary to overcome this issue [12].

Titanium dioxide, a versatile nanomaterial, has a broad multi-functionality, no toxicity, inexpensiveness, and excellent long-term stability, which makes it to use in different fields including pigments in foodstuffs, paint, and cosmetics [13–15]. It became of great interest in the last decades for its photocatalytic properties [16–18]. However, TiO_2 is photoactive only in the near ultraviolet (UV) area. Since the UV region of sunlight is only 3%–4% of the total spectrum, TiO_2 does not utilize solar light very efficiently [19]. Hence, making TiO_2 nanomaterials active in the visible region can enhance its utility as a photocatalyst [20]. TiO_2 nanomaterials have a wide band gap energy and relatively high electron–hole recombination rate, which is contrary to the photocatalytic activity [21]. Therefore, doping with metal oxides capable of reducing band gap energy attracts light response and promotes the separation of holes and electrons [22–24]. For example, because of more concerns to adjust the band gap of semiconductors in order to expand their band gap energy for extending the absorption threshold of TiO_2 bulky powder, the effects of some transitional metal oxides such as W, Mn, Zr, and Cr as dopant have been already investigated [1,25–28]. The presence of such metal oxide dopants in the TiO_2 crystalline significantly influence photoreactivity through shifting the band gap of the catalysts into visible light [29]. Moreover, synthesis of TiO_2 nanomaterials through conventional methods results in agglomeration, low stability, and less dispersion in the medium used [30,31]. Hence, surface modification of nanomaterials using a suitable surfactant or organic ligand or capping agent can be a suitable strategy to overcome the aforementioned defects [17]. In our recently published works, we reported the application of *n*-butylamine as one of the suitable surface modifiers in the synthesis of metal-oxide-doped TiO_2 nanomaterials through mild hydrothermal technique [7]. This method provides suitable conditions for synthesis of nanomaterials in a closed vessel, i.e., general purpose autoclave. This is an eco-friendly, cost-effective, perfect nucleation, and simple method, which could be used for synthesis of metal-oxide-doped nanomaterials [32]. In addition, the hydrothermal method is conducted through an aqueous process, enabling satisfactory solubility, uniform dispersion of doping metal ions, and control of stoichiometry [33].

The objective of this study is to synthesize and characterize surface modified chromium-doped TiO_2 nanoparticles under mild synthetic conditions. The Cr-doped TiO_2 nanoparticles have been synthesized by varying the Cr concentration. In addition, the applicability of the Cr-doped TiO_2 nanoparticles were assessed for the degradation of RB 5 dye under natural sunlight illumination.

2. Materials and methods

2.1. Chemicals

The following chemicals were used as received for the nanomaterials preparation: (i) titanium dioxide TiO_2 (Merck, Germany, gas chromatography (GC) grade with over 99.9% purity), used as precursor; (ii) chromium oxide Cr_2O_3 (Merck, GC grade with 99% purity), used as dopant; (iii) HCl (Merck, guaranteed reagent grade, 37%), used as mineralizer; (iv) *n*-butylamine (Merck, GC grade, 99%), used as surface modifier; and RB5 (Alvan Sabet Co., Iran).

2.2. Synthesis of surface modified Cr-doped TiO_2 nanomaterials

Cr-doped TiO_2 nanomaterials were fabricated under mild hydrothermal conditions at p = autogenous, $T = 100°C$, and $t = 12$ h. In brief synthesis, 1 mol of reagent grade TiO_2 was taken as starting material source for each synthesis and the Cr-doped TiO_2 nanoparticles with different Cr mole ratios were prepared by adding three different mole percentage concentrations of chromium oxide (1, 1.5, and 2 mol%). Approximately, 1 M HCl (10 mL) was taken as a solvent for the mixing of the synthesis precursors. The detailed hydrothermal synthesis procedure for doped TiO_2 nanomaterials with 0.5 mL of *n*-butylamine as a surface modifier was already reported in our previous work [7]. In the present study, we omitted the calcination step.

2.3. Photocatalytic degradation experiments

Photodegradation efficiency of synthesized nanomaterials for the degradation of RB5 was evaluated in aqueous media. The influence of dye concentrations (10–300 mg/L) experimental solutions were prepared by diluting the stock solution with distilled water. The reaction suspension was optimized through adding different amounts (0.5–5.0 g/L) of Cr-doped TiO_2 photocatalyst in 100 mL of dye solution. Prior to the irradiation, the reaction mixture was kept in darkness for 30 min under continuous shaking ($\omega = 100$ rpm) to ensure balanced adsorption–desorption equilibrium. The mixture was then irradiated with the sunlight separately. In order to utilize the sunlight more efficiently each set of experiments was carried out during 12:30 a.m.–2:00 p.m. ($T = 40°C \pm 4°C$). The outdoor experiments were carried out using a 250 mL Pyrex glass reservoir placed on a shaker exposed to the sunlight directly. Throughout all experiments, aeration was maintained by optimal shaking through automatic shaker [34]. All the Pyrex glass reactor containing reaction mixture was covered with a very thin cellophane cover to avoid the mass loss in reactant. For the sake of comparison, a blank experiment was performed at identical experimental conditions. The suspension was sampled at specific time intervals (30, 60, 90, and 120 min) to monitor the changes of RB5 concentration. Suspension sampled (approximately 4 mL) was centrifuged at 4,500 rpm for 30 min to separate out the photocatalyst. Then, supernatant aqueous mixture was analyzed using a double beam UV–Vis spectrophotometer at 597 nm (λ_{max}) corresponding to the maximal absorbance of the dye.

3. Results and discussion

3.1. Characterization of Cr-doped TiO_2 nanomaterials

The surface modified Cr-doped TiO_2 nanomaterials were characterized using an 18-kW advanced X-ray diffractometer (Bruker D8-ADVANCE, Ettlingen, Germany) with Cu K_α radiation (λ = 1.54056 Å). Fig. 1 shows the X-ray diffraction (XRD) plots (2θ: 5°–80°) of the fabricated nanomaterials (where Figs. 1(a), (b), and (c) represent 1, 1.5, and 2 mol% Cr-doped TiO_2 nanomaterials, respectively). As it indicates, the main peaks are present at 25.36°, 37.86°, 48.13°, 53.97°, 55.14°, 62.73°, 68.80°, 70,32°, and 75.13° corresponding to different planes of TiO_2 (JCPDS, number 21-1272) [35]. However, the appearance of new peaks at 44.39° and 64.58° demonstrates the existence of Cr in the TiO_2 structure. The detected metal oxide phases in the patterns suggesting that metal oxide could be existed as crystal phase with incorporating to the TiO_2 lattice, or its goes to the substitutional sites in the TiO_2 lattice [36]. Moreover, the intensities of the peaks were almost the same, indicating that doping did not change their crystallites [37]. In contrary, Ola and Maroto-Valer [38] did not observe chromium peaks in its metal or oxide phase even at the highest loading ratio of 2 mol% within the XRD detection limits. The Scherrer's equation was used for calculating the average crystalline size of each sample (in the range of 60–85 nm) [39]. The results revealed that the incorporation of dopant ions decreased the crystalline size due to the prevention of agglomeration of nanomaterials, which could be attributed to the effect of the surface modifier.

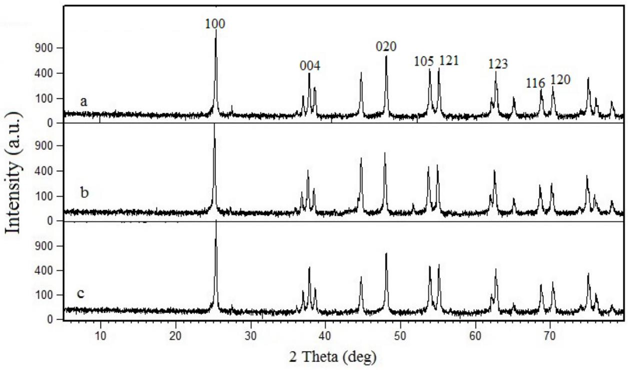

Fig. 1. Powder XRD patterns of: (a) reagent grade TiO_2; (b) 1% Cr-doped TiO_2 nanomaterials; and (c) 2% Cr-doped TiO_2 nanomaterials.

The surface morphology of nanomaterials is another important factor in photodegradation of pollutants. Figs. 2(a)–(c) show the scanning electron microscopy (SEM) images of 1, 1.5, and 2 mol% Cr-doped TiO_2 nanomaterials. Nanoparticles do not have homogenous morphology; the dominant morphology was observed spherical, followed

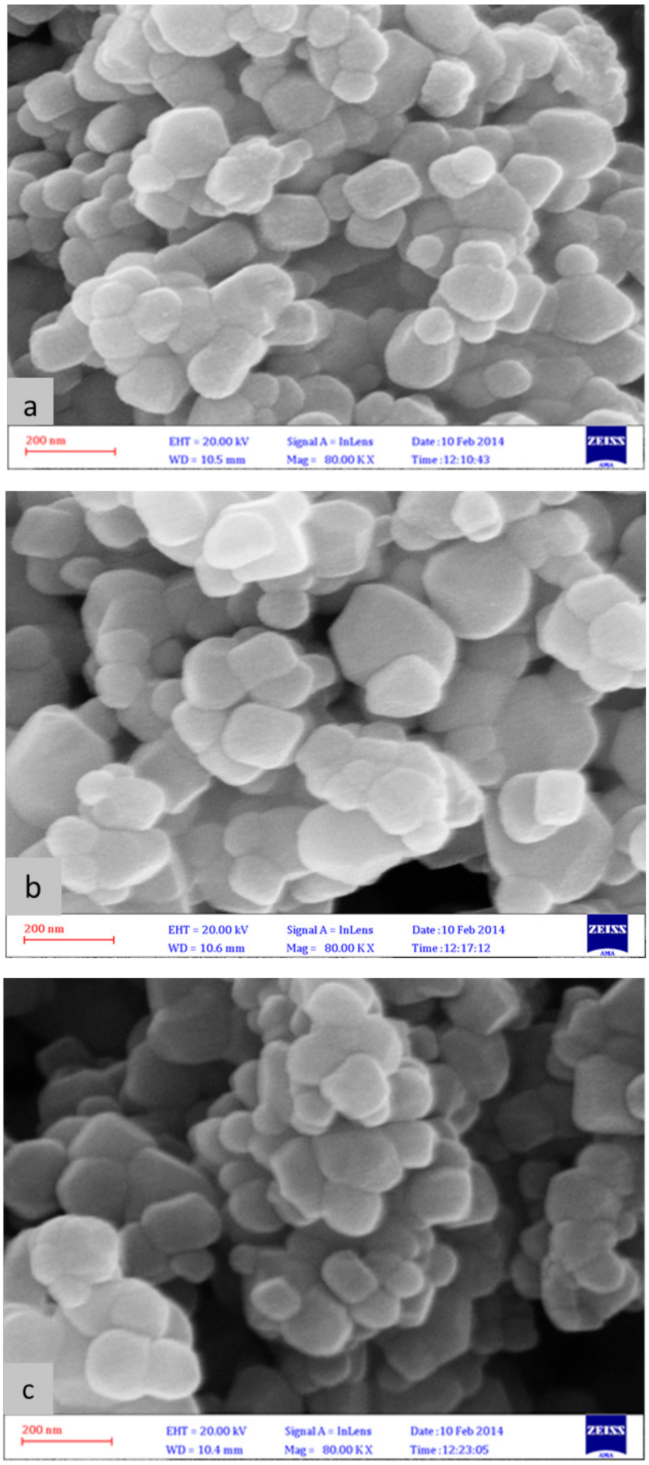

Fig. 2. SEM images of Cr-doped TiO_2 nanomaterials: (a), (b), and (c) represent 1, 1.5, and 2 mol% of Cr, respectively.

by rectangular crystals. Jonidi-Jafari et al. [29] reported that photodegradation of organic dyes using nanosized TiO_2 is depended on the morphology of the fabricated nanomaterials. Energy dispersive X-ray (EDX) spectroscopy elucidates the chemical composition of the synthesized Cr-doped TiO_2 nanomaterials [30]. Fig. 3 shows the characteristic composition peaks obtained for Cr-doped TiO_2 nanomaterials confirming 100% purity of the synthesized material. The EDX profile displayed a strong peak at the energy of 4.5 keV for Ti and some of the weak peaks for Cr and O were observed confirming chromium oxide is well doped in the TiO_2 lattice. Application of surface modifier may result in attachment of some functional groups on the surface of the fabricated nanomaterials. Fig. 4 shows the attenuated total reflection (ATR) spectra of Cr-doped TiO_2 nanomaterials. As Fig. 4 indicates, no new peaks were formed confirming detachment of the surface modifier applied [31].

3.2. Photocatalytic degradation of RB5

A systematic study was conducted on the assessing effect of operational parameters including pH, H_2O_2 concentration, dye initial concentration, nanomaterial dosage, detention time, and light source on the photodegradation of RB5. Natural sunlight illuminance was measured using light meter (LX-101, Lutron Electronic Enterprise Co., Taiwan) at time intervals of 30 min. The average sun illuminance measured was 656.75 lx, while the average UV illuminance measured using an UV radiation meter (Lian Hong CHY 732, Taiwan) was 1.312 mW/cm^2.

Fig. 5 shows the results from RB5 photocatalytic degradation using various Cr-dopant photocatalysts which follows the order of degradation efficiency in the order of 1 > 1.5 > 2 > 0 mol% Cr-doped TiO_2. Similar trend has been previously reported that there exists an optimum doping amount of Cr and for best photocatalytic performance under the irradiation sunlight. The scientific justification for the reason behind the effect of 1 mol% Cr-doped TiO_2 highest efficiency is quite uncertain in our case; this may be due to the difference in textural property behaviors toward RB5 dye structure. The pretests performed results clearly demonstrate that 1.0% Cr-doped TiO_2 nanomaterials had better photodegradation efficiency compared with other three samples. On the other hand, the undoped (bare) TiO_2 had negligible photodegradation properties compared with different Cr-doped TiO_2 nanomaterials. Hence, for the further photodegradation study we only prefer the 1.0% Cr-doped TiO_2 nanomaterials.

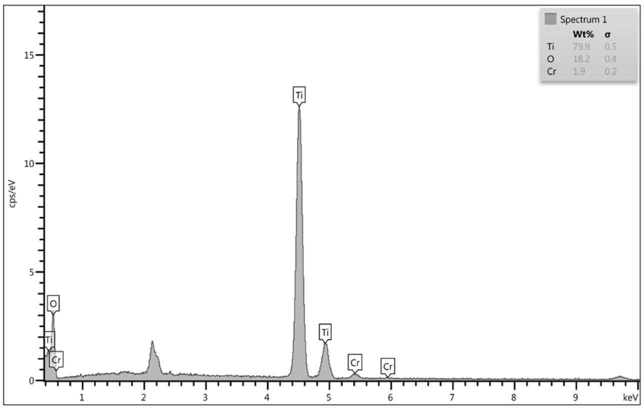

Fig. 3. Characteristic EDX analysis plot of Cr:TiO_2 nanomaterials.

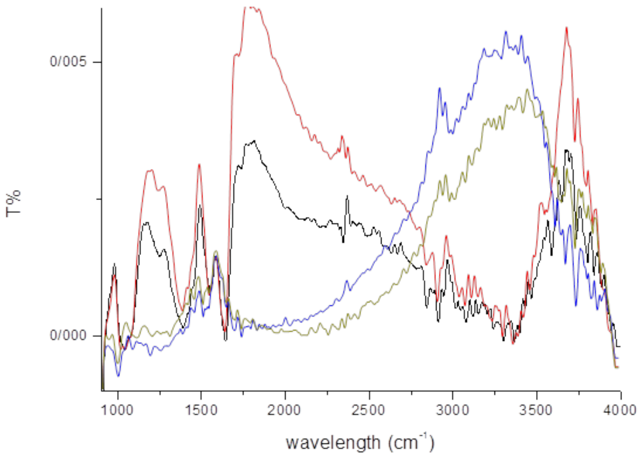

Fig. 4. ATR spectra of — bare TiO_2, — 1 mol% Cr-doped TiO_2, — 1.5 mol% Cr-doped TiO_2, and — 2 mol% Cr-doped TiO_2 nanomaterials.

3.2.1. Effect of pH

It is well known from the previous reports that doping Cr in TiO_2 enhances the degradation efficiency. For this explanation researcher suggested Cr in doped TiO_2 catalyst act as electron remover from hole to decrease electron hole recombination process during the photocatalytic degradation of dyes and responsible to reduce the band gap energy between valence and conduction bands [40]. For this confirmation, we compared the photocatalyst efficiency of bare TiO_2 against degradation of RB5 dye with the influence of pH. The obtained results show less degradation efficiency within wide pH range for bare TiO_2 as was confirmed in Fig. 5.

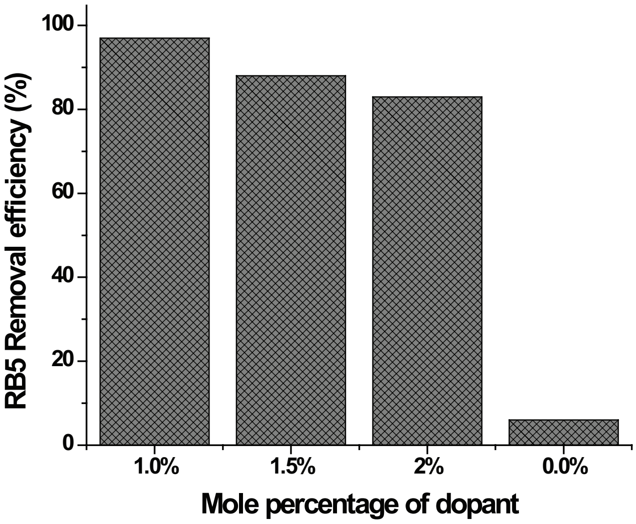

Fig. 5. Effect of dopant molar percentage on the RB5 removal efficiency.

Thus, no further comparison of photodegradation efficiency of Cr-doped TiO_2 was carried out with bare TiO_2. While in the case of Cr-doped TiO_2 material, it shows significant influence of pH by enhanced photocatalytic degradation efficiency. Fig. 6 shows the changes in the pH of dye solutions as a function of the irradiation time for different initial pH values (4, 7, and 10). In general, the point of zero charge (PZC) of various TiO_2 powders is about pH 6 [41]. Above this pH value, the surfaces of TiO_2 particles are negatively charged, which adsorb cationic species readily, while below this pH value they are positively charged which, adsorb anionic species easily. Therefore, the photodegradation efficiency of organic pollutants like RB5 dye in aqueous solution decrease with an increase of pH value above the PZC. Naturally, RB5 has a low p*Ka* value due to the presence of sulfonic group in its chemical structure. It should be expected that the degradation rate constant of RB5 would increase when the pH decreases [42,43]. As Fig. 6 indicates, the minimum and maximum dye removal efficiency occurred at 10 (9.5% after 30 min) and 4 (74.62% after 2 h), respectively. Thus, it can be concluded that the optimum pH for the degradation of RB5 is at pH 4.

3.2.2. Effect of H_2O_2 concentration

The concentration of hydrogen peroxide (H_2O_2) is a crucial parameter affecting the efficiency of dye removal through photodegradation process. Numerous authors have reported that the concentration of H_2O_2 may either enhance the photoreaction rate or inhibit it due to the scavenging action of peroxide, the increase and decrease of the degradation rate also depends on the concentration of peroxide added [44,45]. In order to determine the effect of H_2O_2 concentration on the RB5 degradation rate, the amount of H_2O_2 in the range of 5–50 mmol was added. Fig. 7 shows plots for RB5 photodegradation efficiency vs. different concentrations of H_2O_2. The obtained results explore that the photodegradation efficiency increased from 62.5% to 87.5% as the H_2O_2 concentration increased from 5 to 20 mmol. However, further increasing H_2O_2 concentration to 20 mmol, the photodegradation efficiency reached a plateau and stayed almost unchangeable (61%). The findings displayed the existence of an optimal molar ratio between peroxide and dye that leads to a faster decolorization rate. The similar type of results was also observed by Mitrovic et al. [46]; they reported that 25 mmol of H_2O_2 was found the optimum concentration for the removal of reactive orange dye. Here from our observation, in this study we concluded that 20 mmol of H_2O_2 concentration was the optimum concentration and was utilized for further study.

3.2.3. Effect of photocatalyst loading

The required concentration of Cr-doped TiO_2 nanomaterials for the decolorization of a 50 mg/L RB5 dye solution was scrutinized with the slurry method by varying the quantities of nanoparticles amount (0.5, 1.0, 1.5, 2.0, 3.0, and 5.0 g/L). In contrary to our pervious observation [9,18], photodegradation efficiency of RB5 was proportional with increasing Cr-doped TiO_2 nanomaterials dosage (Fig. 8). Active hydroxyl radicals

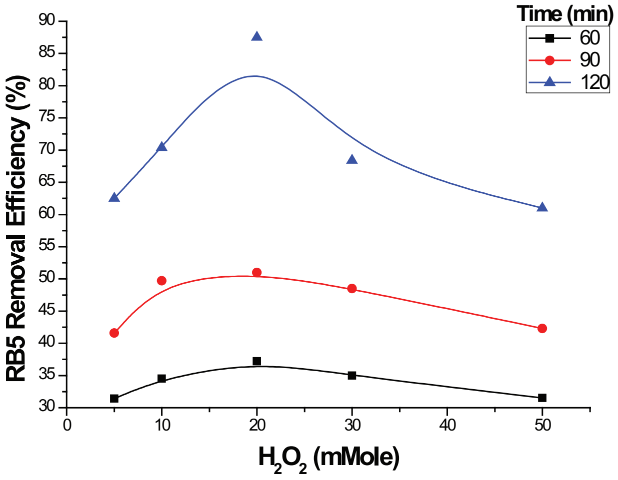

Fig. 7. Effect of H_2O_2 concentration on the photodegradation efficiency of RB5 (pH = 4, Cr-doped TiO_2 dosage = 1.0 g/L, dye concentration = 50 mg/L under sunlight illumination).

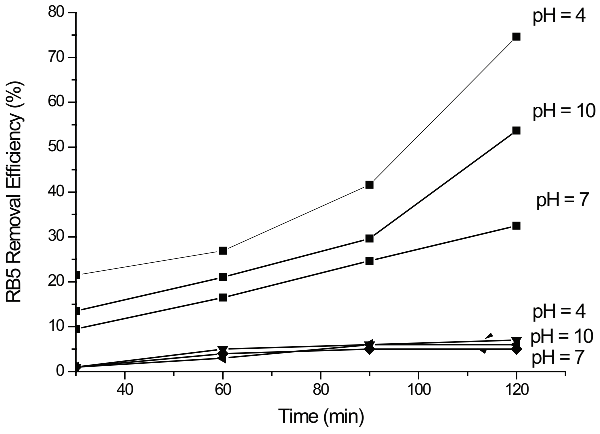

Fig. 6. Effect of pH on the RB5 removal efficiency using H_2O_2 = 15 mL, dye concentration = 50 mg/L, and 1 g/L nanomaterials under sunlight illumination (■ Cr-doped TiO_2, ▼ bare TiO_2).

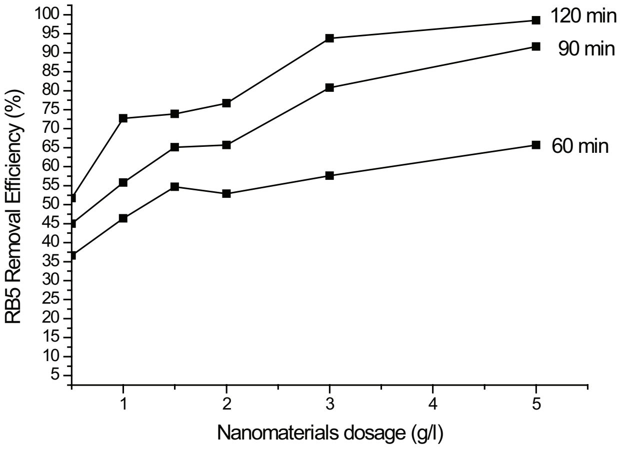

Fig. 8. Effect of Cr-doped TiO_2 nanoparticles dosage on the photodegradation efficiency of RB5 (pH = 4, H_2O_2 concentration = 20 mM, dye concentration = 50 mg/L under sunlight irradiation).

could contribute such effect because of the presence of highest active site for the attack of heavier molecules [47]. Zaidill Azizan et al. [48] reported 99% efficiency for RB5 decolorization using Fe-areca nut as a heterogeneous Fenton catalyst. However, in the present study we utilized natural sunlight as a freely available source of energy, which could justify such comparatively lower degradation efficiency.

3.2.4. Effect of the initial dye concentration

Initial dye concentration is one of the most important parameters that can affect the photoreaction rate of photocatalysis process [49]. Dye solutions of 10, 25, 50, 100, 200, and 300 mg/L were used for studying the effect of initial dye concentration on the photodegradation efficiency of RB5. Fig. 9 demonstrates that initial dye concentration has a significant effect on the dye removal. The higher initial concentration of dye solution, and the lower photodegradation efficiency [50]. This effect could be well explained by chemical structure of RB5. It has a complex structure and two azo bonds; therefore, at stable condition of other parameters the increases of the initial dye concentration show the dye removal decreased. Moreover, at all of the abovementioned steps, photodegradation process was found to be time depended on the time treatment.

3.2.5. Possible dye degradation mechanism

A semiconductor photocatalytic reaction is originated when photoelectrons are stimulated from the valence band to the empty conduction band due to various types of energy irradiations. The absorbed photon has energy (*h*ν), which is either equal to or greater than the band gap of the specific semiconductor photocatalyst. The excitation process results a hole in the valence band (h_{VB}^+) and as a net results, electron and hole pair (e^-/h^+). The photogenerated hole pair at the valence band then react with water to produce hydroxyl radicals. The hydroxyl radicals generated are extremely powerful oxidizing agent. It attacks adsorbed organic molecules causing them to degrade their structure and stability. In case of bare TiO_2 photocatalyst the distance between valence and conduction band is too large (3.31 eV), in such cases adsorption of visible light is negligible and hence it results in poor photocatalytic activity of bare TiO_2 against the degradations of various dyes in aqueous medium. On the other hand, in case of Cr-doped TiO_2 photocatalyst due to depended material properties – which generate extra valence band – which is convenient for the visible light absorption, hydroxyl radical's formation, and simultaneously responsible for radical initiated degradation mechanism of dye (RB5).

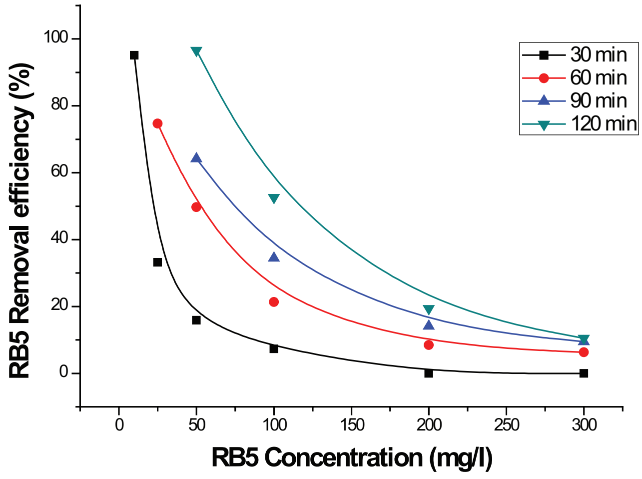

Fig. 9. Effect of initial dye concentration on the photodegradation efficiency of RB5 (pH = 4, H_2O_2 concentration = 20 mM, Cr-doped TiO_2 nanomaterials dosage = 5.0 g/L under sunlight illumination).

4. Conclusions

Using *n*-butylamine as surface modifier, chromium-doped TiO_2 nanomaterials were synthesized under mild hydrothermal conditions. The characterization results indicated excellent morphology, high crystallinity, and purity of the Cr-dopant nanomaterials. ATR analysis revealed detachment of *n*-butylamine from the surface of nanoparticles. In the present study, the potential capabilities of the nanomaterials synthesized (Cr-doped TiO_2 nanomaterials) as an eco-friendly catalyst for the removal of RB5 from aqueous solution was demonstrated. The degree of decolorization of RB5 was affected by Cr-doped TiO_2 nanomaterials dosage, pH, H_2O_2 concentration, and initial dye concentration. The systematic study for optimization of various parameters conclude that 5.0 g/L of Cr-doped TiO_2 nanomaterials, pH 4, H_2O_2 20.0 mmol, and 120 min of contact time are the optimized conditions for the degradation of 96.6% of 50 mg/L RB5 dye in the presence of natural sunlight. In addition, this study supports that doping TiO_2 with a suitable metal oxide such as chromium could induce photodegradation efficiency under natural sunlight illumination and fabricated Cr-doped TiO_2 nanomaterials could be a good candidate for photodegradation of complex dyes such as RB5.

Acknowledgment

The authors are thankful to the Kermanshah University of Medical Sciences, Kermanshah, Iran, for financial support.

References

[1] M. Shirzad Siboni, M.T. Samadi, J.K. Yang, S.M. Lee, Photocatalytic reduction of Cr(VI) and Ni(II) in aqueous solution by synthesized nanoparticle ZnO under ultraviolet light irradiation: a kinetic study, Environ. Technol., 32 (2011) 1573–1579.

[2] A.S. Bhatt, P.L. Sakaria, M. Vasudevan, R.R. Pawar, N. Sudheesh, H.C. Bajaj, H.M. Mody, Adsorption of an anionic dye from aqueous medium by organoclays: equilibrium modeling, kinetic and thermodynamic exploration, RSC Adv., 2 (2012) 8663–8671.

[3] S.-S. Mehdi, K. Alireza, V. Behrouz, W.J. Sang, F. Sevda, Preparation of a green photocatalyst by immobilization of synthesized ZnO nanosheets on scallop shell for degradation of an azo dye, Curr. Nanosci., 10 (2014) 684–694.

[4] M. Farrokhi, S.-C. Hosseini, J.-K. Yang, M. Shirzad-Siboni, Application of ZnO–Fe_3O_4 nanocomposite on the removal of azo dye from aqueous solutions: kinetics and equilibrium studies, Water Air Soil Pollut., 225 (2014) 1–12.

[5] C.D. Raman, S. Kanmani, Textile dye degradation using nano zero valent iron: a review, J. Environ. Manage., 177 (2016) 341–355.

[6] A. Mohagheghian, S.-A. Karimi, J.-K. Yang, M. Shirzad-Siboni, Photocatalytic degradation of a textile dye by illuminated tungsten oxide nanopowder, J. Adv. Oxid. Technol., 18 (2015) 61–68.
[7] B. Shahmoradi, A. Maleki, K. Byrappa, Removal of Disperse Orange 25 using *in situ* surface-modified iron-doped TiO_2 nanoparticles, Desal. Wat. Treat., 53 (2013) 3615–3622.
[8] C. Tang, V. Chen, The photocatalytic degradation of reactive black 5 using TiO_2/UV in an annular photoreactor, Water Res., 38 (2004) 2775–2781.
[9] S.-J. You, R.A. Damodar, S.-C. Hou, Degradation of Reactive Black 5 dye using anaerobic/aerobic membrane bioreactor (MBR) and photochemical membrane reactor, J. Hazard. Mater., 177 (2010) 1112–1118.
[10] M.S. Siboni, M. Samarghandi, J.-K. Yang, S.-M. Lee, Photocatalytic removal of reactive black-5 dye from aqueous solution by UV irradiation in aqueous TiO_2: equilibrium and kinetics study, J. Adv. Oxid. Technol., 14 (2011) 302–307.
[11] O.B. Ayodele, O.S. Togunwa, Catalytic activity of copper modified bentonite supported ferrioxalate on the aqueous degradation and kinetics of mineralization of Direct Blue 71, Acid Green 25 and Reactive Blue 4 in photo-Fenton process, Appl. Catal., A, 470 (2014) 285–293.
[12] W.-K. Jo, R.J. Tayade, Facile photocatalytic reactor development using nano-TiO_2 immobilized mosquito net and energy efficient UVLED for industrial dyes effluent treatment, J. Environ. Chem. Eng., 4 (2016) 319–327.
[13] T. Umebayashi, T. Yamaki, H. Itoh, K. Asai, Analysis of electronic structures of 3d transition metal-doped TiO_2 based on band calculations, J. Phys. Chem. Solids, 63 (2002) 1909–1920.
[14] J.K. Yang, S.M. Lee, M. Farrokhi, O. Giahi, M. Shirzad Siboni, Photocatalytic removal of Cr(VI) with illuminated TiO_2, Desal. Wat. Treat., 46 (2012) 375–380.
[15] M. Shirzad Siboni, M.-T. Samadi, J.-K. Yang, S.-M. Lee, Photocatalytic removal of Cr(VI) and Ni(II) by UV/TiO_2: kinetic study, Desal. Wat. Treat., 40 (2012) 77–83.
[16] A. Ghicov, B. Schmidt, J. Kunze, P. Schmuki, Photoresponse in the visible range from Cr doped TiO_2 nanotubes, Chem. Phys. Lett., 433 (2007) 323–326.
[17] J.K. Yang, S.M. Lee, M.S. Siboni, Effect of different types of organic compounds on the photocatalytic reduction of Cr(VI), Environ. Technol., 33 (2012) 2027–2032.
[18] M. Shirzad-Siboni, M. Farrokhi, R. Darvishi Cheshmeh Soltani, A. Khataee, S. Tajassosi, Photocatalytic reduction of hexavalent chromium over ZnO nanorods immobilized on kaolin, Ind. Eng. Chem. Res., 53 (2014) 1079–1087.
[19] B. Shahmoradi, M. Negahdary, A. Maleki, Hydrothermal synthesis of surface-modified, manganese-doped TiO_2 nanoparticles for photodegradation of methylene blue, Environ. Eng. Sci., 29 (2012) 1032–1037.
[20] M.M. Khan, S.A. Ansari, D. Pradhan, M.O. Ansari, D.H. Han, J. Lee, M.H. Cho, Band gap engineered TiO_2 nanoparticles for visible light induced photoelectrochemical and photocatalytic studies, J. Mater. Chem. A, 2 (2014) 637–644.
[21] M. Farrokhi, J.-K. Yang, S.-M. Lee, M. Shirzad-Siboni, Effect of organic matter on cyanide removal by illuminated titanium dioxide or zinc oxide nanoparticles, J. Environ. Health Sci. Eng., 11 (2013) 23.
[22] Z. Yao, F. Jia, Y. Jiang, C. Li, Z. Jiang, X. Bai, Photocatalytic reduction of potassium chromate by Zn-doped TiO_2/Ti film catalyst, Appl. Surf. Sci., 256 (2010) 1793–1797.
[23] B.H. Nguyen, V.H. Nguyen, D.L. Vu, Photocatalytic composites based on titania nanoparticles and carbon nanomaterials, Adv. Nat. Sci.: Nanosci. Nanotechnol., 6 (2015) 033001.
[24] Y. Hu, J. Shi, L. Guo, Enhanced photocatalytic hydrogen production activity of chromium doped lead niobate under visible-light irradiation, Appl. Catal., A, 468 (2013) 403–409.
[25] X. Li, Y. Liu, P. Yang, Y. Shi, Visible light-driven photocatalysis of W, N co-doped TiO_2, Particuology, 11 (2013) 732–736.
[26] W. Zhang, W. Zhou, J.H. Wright, Y.N. Kim, D. Liu, X. Xiao, Mn-doped TiO_2 nanosheet-based spheres as anode materials for lithium-ion batteries with high performance at elevated temperatures, ACS Appl. Mater. Interfaces, 6 (2014) 7292–7300.
[27] Y. Wang, R. Zhang, J. Li, L. Li, S. Lin, First-principles study on transition metal-doped anatase TiO_2, Nanoscale Res. Lett., 9 (2014) 46.
[28] J. Choina, C. Fischer, G.U. Flechsig, H. Kosslick, V.A. Tuan, N.D. Tuyen, N.A. Tuyen, A. Schulz, Photocatalytic properties of Zr-doped titania in the degradation of the pharmaceutical ibuprofen, J. Photochem. Photobiol., A, 274 (2014) 108–116.
[29] A. Jonidi-Jafari, M. Shirzad-Siboni, J.-K. Yang, M. Naimi-Joubani, M. Farrokhi, Photocatalytic degradation of diazinon with illuminated ZnO–TiO_2 composite, J. Taiwan Inst. Chem. Eng., 50 (2015) 100–107.
[30] K. Byrappa, T. Adschiri, Hydrothermal technology for nanotechnology, Prog. Cryst. Growth Charact. Mater., 53 (2007) 117–166.
[31] M. Naimi-Joubani, M. Shirzad-Siboni, J.-K. Yang, M. Gholami, M. Farzadkia, Photocatalytic reduction of hexavalent chromium with illuminated ZnO/TiO_2 composite, J. Ind. Eng. Chem., 22 (2015) 317–323.
[32] B. Shahmoradi, K. Byrappa, A. Maleki, Hydrothermal Modification of Metal Oxide-Doped TiO_2 Nanomaterials, M. Aliofkhazraei, Ed., Handbook of Functional Nanomaterials: Characterization and Reliability, Nova Science Publishers, New York, USA, 2013.
[33] H. Feng, M.-H. Zhang, L.E. Yu, Hydrothermal synthesis and photocatalytic performance of metal-ions doped TiO_2, Appl. Catal., A, 413–414 (2012) 238–244.
[34] M.A. Nawi, I. Nawawi, Preparation and characterization of TiO_2 coated with a thin carbon layer for enhanced photocatalytic activity under fluorescent lamp and solar light irradiations, Appl. Catal., A, 453 (2013) 80–91.
[35] X. Li, W. Li, M. Li, P. Cui, D. Chen, T. Gengenbach, L. Chu, H. Liu, G. Song, Glucose-assisted synthesis of the hierarchical TiO_2 nanowire@MoS_2 nanosheet nanocomposite and its synergistic lithium storage performance, J. Mater. Chem. A, 3 (2015) 2762–2769.
[36] M. Pawar, V. Nimbalkar, Synthesis and phenol degradation activity of Zn and Cr doped TiO_2 nanoparticles, Res. J. Chem. Sci., 2 (2012) 32–37.
[37] A. Tuan Vu, Q. Tuan Nguyen, T.H. Linh Bui, M. Cuong Tran, T. Phuong Dang, T.K. Hoa Tran, Synthesis and characterization of TiO_2 photocatalyst doped by transition metal ions (Fe^{3+}, Cr^{3+} and V^{5+}), Adv. Nat. Sci.: Nanosci. Nanotechnol., 1 (2010) 015009.
[38] O. Ola, M.M. Maroto-Valer, Transition metal oxide based TiO_2 nanoparticles for visible light induced CO_2 photoreduction, Appl. Catal., A, 502 (2015) 114–121.
[39] P. Bindu, S. Thomas, Estimation of lattice strain in ZnO nanoparticles: X-ray peak profile analysis, J. Theor. Appl. Phys., 8 (2014) 123–134.
[40] Y.L. Wei, K.W. Chen, H.P. Wang, Study of chromium modified TiO_2 nano catalyst under visible light irradiation, J. Nanosci. Nanotechnol., 10 (2010) 5456–5460.
[41] A. Ajmal, I. Majeed, R.N. Malik, H. Idriss, M.A. Nadeem, Principles and mechanisms of photocatalytic dye degradation on TiO_2 based photocatalysts: a comparative overview, RSC Adv., 4 (2014) 37003.
[42] M.N. Chong, Y.J. Cho, P.E. Poh, B. Jin, Evaluation of Titanium dioxide photocatalytic technology for the treatment of reactive Black 5 dye in synthetic and real greywater effluents, J. Cleaner Prod., 89 (2015) 196–202.
[43] L. Xu, X. Li, J. Ma, Y. Wen, W. Liu, Nano-MnO_x on activated carbon prepared by hydrothermal process for fast and highly efficient degradation of azo dyes, Appl. Catal., A, 485 (2014) 91–98.
[44] R.R. Giri, H. Ozaki, Y. Takayanagi, S. Taniguchi, R. Takanami, Efficacy of ultraviolet radiation and hydrogen peroxide oxidation to eliminate large number of pharmaceutical compounds in mixed solution, Int. J. Environ. Sci. Technol., 8 (2010) 19–30.
[45] Y. Xiao, L. Zhang, J. Yue, R.D. Webster, T.-T. Lim, Kinetic modeling and energy efficiency of UV/H_2O_2 treatment of iodinated trihalomethanes, Water Res., 75 (2015) 259–269.
[46] J. Mitrovic, M. Radovic, D. Bojic, T. Andjelkovic, M. Purenovic, A. Bojic, Decolorization of textile azo dye reactive orange 16 with UV/H_2O_2 process, J. Serb. Chem. Soc., 77 (2012) 465–481.

[47] K. Santhi, P. Manikandan, C. Rani, S. Karuppuchamy, Synthesis of nanocrystalline titanium dioxide for photodegradation treatment of remazol brown dye, Appl Nanosci., 5 (2014) 373–378.

[48] M.A. Zaidill Azizan, H. Hassan, S. Faraziehan, N. Abu Hassan, Decolorization of Reactive Black 5 using Fe-areca nut as a heterogeneous Fenton catalyst, Appl. Mech. Mater., 661 (2014) 29–33.

[49] S. Laohaprapanon, J. Matahum, L. Tayo, S.-J. You, Photodegradation of Reactive Black 5 in a ZnO/UV slurry membrane reactor, J. Taiwan Inst. Chem. Eng., 49 (2015) 136–141.

[50] E. Kafshdare Goharshadi, M. Hadadian, M. Karimi, H. Azizi-Toupkanloo, Photocatalytic degradation of reactive black 5 azo dye by zinc sulfide quantum dots prepared by a sonochemical method, Mater. Sci. Semicond. Process., 16 (2013) 1109–1116.